

AN ALTERNATIVE WAY TO THE PWM CONTROL OF SWITCHED RELUCTANCE MOTOR DRIVES

Hedi YAHIA^(a), Mohamed Faouzi MIMOUNI^(b), Rachid DHIFAOUI

^(a)Engineering School of Monastir 5019 Tunisia

^(b)Engineering School of Monastir 5019 Monastir Tunisia

^(c)Institute of Applied Science 3012 Tunis Tunisia

^(a)Hedi.Yahia@enim.rnu.tn, ^(b)MFaouzi.Mimouni@enim.rnu.tn, ^(c)Rachid.Dhifaoui@insat.rnu.tn

ABSTRACT

The paper presents one alternative method to the conventional PWM control that provides high performance at low speed. The new developed control concept can significantly accomplish the performance of the SRM in terms of efficiency, torque ripple and power quality when compared to standard PWM current control. This control consists of feeding each phase with a constant volt per hertz (V/f) law for low speed range. The suggested V/f method is simple and is easy for practical implementation. Principle of this mode of control and analytical expressions for current calculation are provided and discussed. Obtained simulation results demonstrate the effectiveness of the proposed control strategy.

Keywords: PWM current control, single pulse, switched reluctance machine, V/f.

1. INTRODUCTION

By construction, the SRM is the simplest of all electrical machines. Only the stator has windings. The rotor contains no conductors or permanent magnets. It consists simply of steel laminations stacked onto a shaft. Motion is produced by the variation of the reluctance in the air gap between the rotor and the stator. The simple mechanical construction is one of the main attractive features which have motivated a large amount of research on SRM (Pillay et al 1997). One of the drawbacks of the SRM is the relatively large torque ripple when controlled by basic control strategies as compared to other types of electric machines (Mademlis and Kioskeridis 2003). This large torque ripple produces intensive and undesirable vibration and acoustic noise and limits the application areas of SRM (Venkatesha and Ramanarayanan 1998).

To reduce these disadvantages, most of the published papers are supported by exhaustive measurements of SRM magnetic characteristics. Sophisticated nonlinear adaptive control schemes of SRM have also been proposed (Henriques et al 2002, Zhang et al 2009). The disadvantages of these methods are that they are complex and computationally expensive which makes real-time implementation

difficult (Russa et al 1997). To maintain SRM drives at low cost, there is a need for an easy to implement and cost-effective control method that provides acceptable performance over a wide speed range (David and Fukuda 2002).

There are several parameters for controlling SRM, such as turn-on angle, turn-off angle, and exciting voltage and controlling mode. In this paper, a novel control method that applies V/f law is developed. The optimal turn-on angle is fine-tuned referring to conventional control method. The optimal turn-off angle is defined at the critical rotor position where the current of next winding phase reaches its desired value (Kioskeridis and Mademlis 2007).

The purpose of this paper is to propose a novel strategy of control for SRM drives, which entirely operates on single-pulse mode. Variable DC voltage and full DC voltage are available for magnetization and demagnetization purposes respectively. The model and the basic equations of the SRM are first explained. This is followed by the presentation of the control parameters. The effectiveness of the proposed strategy is assessed by comparing the simulation results of the novel strategy with the PWM control. Finally, conclusions are given.

2. MATHEMATICAL MODEL OF SRM AND CURRENT ANALYSIS

2.1. Linear Math Model

The SRM used in this study is an 8/6 SRM Oulton with split dc supply converter. We model SRM in the linear region and we neglect effect of mutual inductances. The idealized obtained inductance profile for one phase is shown by Figure 1. The significant inductance profile changes are determined in terms of the stator and rotor pole-arcs and number of rotor poles (Krishnan 1994). The various angles are derived as follows. In this set of equations, β_s and β_r are stator and rotor pole-arcs, respectively. N_r is the number of rotor poles.

$$\begin{cases} \theta_1 = \frac{1}{2} \left[\frac{2\pi}{N_r} - (\beta_s + \beta_r) \right] \\ \theta_2 = \theta_1 + \beta_s \\ \theta_3 = \theta_2 + (\beta_s + \beta_r) \\ \theta_4 = \theta_3 + \beta_s \\ \theta_5 = \theta_2 + \theta_1 = \frac{2\pi}{N_r} \end{cases} \quad (1)$$

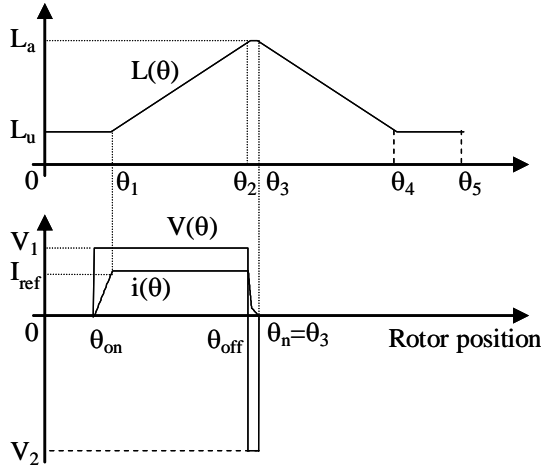


Figure 1: Idealized inductance profile vs. rotor position of a SRM

During rotor running, inductance changes from the minimum L_u to the maximum L_a periodically. L_u occurs when the axis of the rotor pole is aligned with axis passing by the center of the stator pole. On the other hand, maximum inductance L_a corresponds to the situation where the axes of rotor pole and stator pole are in the same position. The relationship between inductance $L(\theta)$ and the position θ of the rotor can be shown through the following function (Zai-ping and Hu 2004).

$$L(\theta) = \begin{cases} L_u & 0 \leq \theta \leq \theta_1 \\ L_u + L_s(\theta - \theta_1) & \theta_1 \leq \theta \leq \theta_2 \\ L_a & \theta_2 \leq \theta < \theta_3 \\ L_a - L_s(\theta - \theta_3) & \theta_3 \leq \theta \leq \theta_4 \\ L_u & \theta_4 \leq \theta < \theta_5 \end{cases} \quad (2)$$

Among the functions, $L_s = \frac{L_a - L_u}{\theta_2 - \theta_1}$ is the slope increasing inductance.

2.2. Converter Configuration

SRM converter configuration is a split dc converter as shown in Figure 2. The phase A is energized by turning on transistor T_1 . In this step, the current flows through transistor T_1 , phase winding A and the capacitor C_1 .

When T_1 is turned off, the current will continue to flow (decreasing phase) through phase winding A, diode D_1 , and capacitor C_2 . Similar operations follow for phases B, C, and D. During increasing interval when T_1 is on, the winding phase voltage is V_1 whose amplitude is proportional to the reference speed. During decreasing interval when T_1 is off, the winding phase voltage is V_2 whose amplitude is kept constant to the rated value. When the speed becomes higher than the rated value, the voltage magnitude of V_1 is also kept to the rated value. More care has to be exercised in balancing the charges of C_1 and C_2 by adequate design measures (Ertl and Kolar 2008, Lee et al 2006). Here, to satisfy the functional requirements of C_1 and C_2 neutral point and variable voltage of V_1 , a three phase, four wire semi-controlled rectifier topology is proposed in Figure 3.

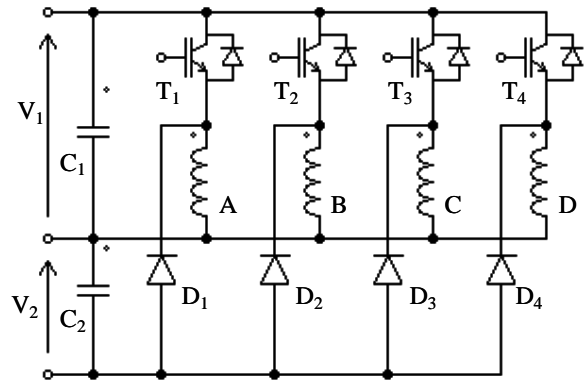


Figure 2: Split dc converter topology of a four-phase SRM

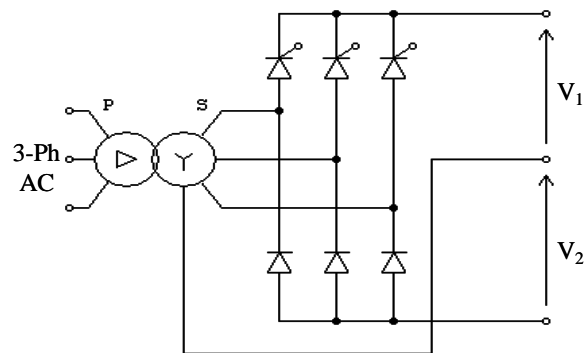


Figure 3: Three phase, four wire semi-controlled rectifier

2.3. Current Analysis

Figure 1 indicates that $dL/d\theta$ is negative for $\theta > \theta_3$. To avoid any negative torque production, equation 5 indicates that the phase current should be regulated to zero before reaching θ_3 . On the other hand, to ensure instantaneous torque production, it is essential that the

phase current is expected to reach a high value when inductance begins to increase. This means that the stator phase winding should be excited between 0 and θ_1 .

Analysis of current shape considered in Fig. 1 is based on the following electrical equation where θ is the electrical angle, ω is the angular speed, R is the phase resistance, and V is the phase voltage. The mutual flux between the phases is assumed to be zero.

$$V = iR + \frac{d\Phi(\theta, i)}{dt} = iR + \frac{d\Phi(\theta, i)}{d\theta} \omega + \frac{d\Phi(\theta, i)}{di} \frac{di}{dt} \quad (3)$$

For the linear phase inductance model adopted in this study, (3) can be rewritten as follows where $L(\theta)$ is given in Fig. 1.

$$V = iR + \frac{d}{dt} [iL(\theta)] = iR + i\omega \frac{dL(\theta)}{d\theta} + L(\theta) \frac{di}{dt} \quad (4)$$

The developed torque in the n^{th} phase is given by (5). The total torque is then equal to the sum of the contributions from the 4 phases, (6).

$$T_{en} = \frac{1}{2} i_n^2 \frac{dL_n(\theta)}{d\theta} \quad (5)$$

$$T_e = \sum_1^4 T_{en} \quad (6)$$

According to the above, the change of phase current can be divided in four stages assuming constant speed and zero current initial condition $i(\theta_{on})=0$. Solving (4) analytically, current's change can be expressed by the following functions

- Starting phase $\theta_{on} \leq \theta \leq \theta_1$;

$$i(\theta) = \frac{V_1}{R} \left[1 - \exp\left(\frac{R(\theta_{on} - \theta)}{\omega L_u}\right) \right] \quad (7)$$

- Holding phase $\theta_1 \leq \theta \leq \theta_{off}$;

$$i(\theta) = \frac{V_1}{R + \omega L_s} + \left[I(\theta_1) - \frac{V_1}{R + \omega L_s} \right] \left[\frac{L_u}{L_u + L_s(\theta - \theta_1)} \right]^{(1 + \frac{R}{\omega L_s})} \quad (8)$$

- Decreasing phase on positive slope of inductance $\theta_{off} \leq \theta \leq \theta_2$;

$$i(\theta) = \frac{V_2}{R + \omega L_s} + \left[I(\theta_{off}) - \frac{V_2}{R + \omega L_s} \right] \left[\frac{L_u}{L_u + L_s(\theta - \theta_{off})} \right]^{(1 + \frac{R}{\omega L_s})} \quad (9)$$

- Continued decreasing phase in aligned position $\theta_2 \leq \theta \leq \theta_3$.

$$i(\theta) = \frac{V_2}{R} + \left[I(\theta_2) - \frac{V_2}{R} \right] \left[\exp\left(\frac{R(\theta_2 - \theta)}{\omega L_a}\right) \right] \quad (10)$$

3. DEFINING THE CONTROL PARAMETERS

The proposed control is operated in a single pulse mode over the whole speed range of the motor. The current amplitude is controlled by tuning the voltage level and commutation angle θ_{on} according to the desired motor speed. The commutation angles θ_{off} are adjusted to values causing an appropriate duration of the demagnetizing interval to occur at the aligned region (Kioskeridis and Mademlis 2006).

3.1. Selected Turn-on and Turn-off Angles

The analytical expression for determining the turn-on and turn-off angles is adopted in this paper.

We select the turn-on angle so that the phase current reaches its reference value I_{ref} at the angle θ_1 . Thus, we establish on the basis of (3)

$$\theta_{on} = \theta_1 + \frac{\omega L_s}{R} \text{Log} \left(1 - I_{ref} \frac{R}{V_1} \right) \quad (11)$$

Turn-off angle value is usually variable and depends on the motor speed and electromagnetic torque. Here, we consider variable turn-off angle. To inhibit the uprising of a negative torque in the zone of decreasing inductance, θ_{off} is limited to θ_2 in low speed range. Otherwise, θ_{off} limit must be decreased to fulfill the constraint $\theta_e = \theta_3$ which ensures the extinction of the phase current.

During the aligned zone θ_2 – θ_3 , phase current is expressed by (4) which depend upon the current acquired at angle θ_2 . Solving (4) for initial condition $I(\theta_2)$ yields the equation,

$$I(\theta_2) = \frac{V_2}{R} \left(1 - \exp\left(\frac{-R(\theta_2 - \theta_3)}{\omega L_a}\right) \right) \quad (12)$$

In demagnetization period $\theta_{off} - \theta_2$, since full negative voltage V_2 is supplied to motor winding, phase current is fast decreased and is given by (3). On intersection angle θ_2 , the current values obtained by (3) and (4) are equal, thus

$$\frac{V_2}{R} \left[1 - \exp\left(\frac{-R(\theta_2 - \theta_3)}{\omega L_a}\right) \right] = \frac{V_2}{R + \omega L_s} + \left[I(\theta_{off}) - \frac{V_2}{R + \omega L_s} \right] \left[\frac{L_u}{L_u + L_s(\theta_2 - \theta_{off})} \right]^{(1 + \frac{R}{\omega L_s})} \quad (13)$$

The turn-off angle is obtained by solving (13), yielding,

$$\theta_{off} = \theta_2 + \left\{ 1 - \frac{\left[\frac{I(\theta_{off}) - \frac{V_2}{R + \omega L_s}}{\frac{\omega L_s}{R + \omega L_s}} \right]}{\left[\frac{I(\theta_2) - \frac{V_2}{R + \omega L_s}}{\frac{\omega L_s}{R + \omega L_s}} \right]} \right\} \frac{L_u}{L_s} \quad (14)$$

where $I(\theta_{off})$ is equal to I_{ref} .

The above conditions are applied for SRM single-pulse operation. The effect of adopted turn-off angle on the total torque produced is observed in Figure 4. It can be seen that the torque ripple is very significantly increased. To keep the torque ripple level low, it appears preferable to commute around another rotor position, where next winding phase reaches its respective reference value I_{ref} at the angle $\theta_1 + \pi/2$. The new extinguishing angle θ_e is given by (15) and typical torque waveforms for the same mechanical speed ω_r are sketched in Figure 5. We observe an effective amelioration.

$$\theta_e = \theta_{off} + \frac{L_u}{L_s} \left\{ \left[\frac{V_2 - I_{Max}(R + \omega L_s)}{V_2} \right]^{\frac{\omega L_s}{R + \omega L_s}} - 1 \right\} \quad (15)$$

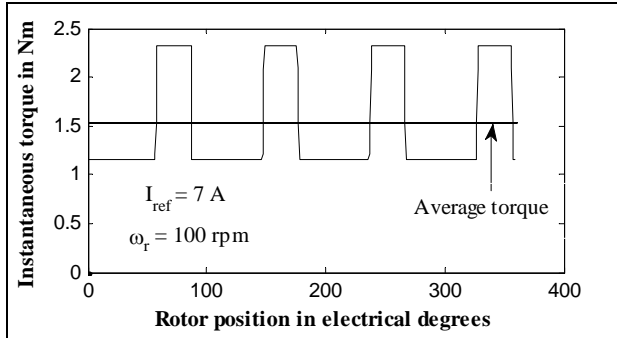


Figure 4: Developed torque with commutation angle θ_{off} calculated from (14)

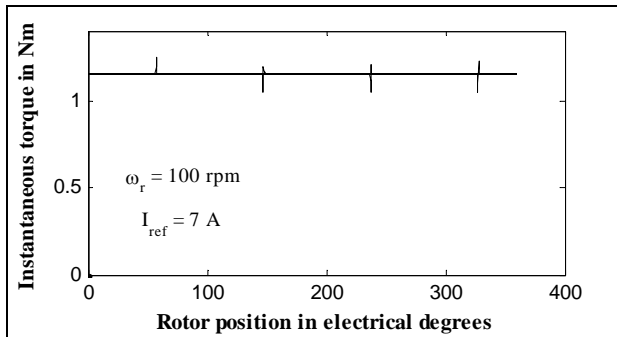


Figure 5: Developed torque with commutation angle $\theta_{off} = \theta_1 + \pi/2$

3.2. Selected V/f Slope

Assume the speed of the machine is constant and neglect the voltage drop across the stator resistance. The

rate of change of phase current can be derived from (4) as follow

$$\frac{di}{dt} = \frac{V - E}{L(\theta)} \quad (16)$$

where $E = i\omega \frac{dL(\theta)}{dt}$ corresponds to the back-EMF.

The behavior of the phase current depends on the relationship between the back-EMF and the source voltage V_1 . An uncontrollable rise of the phase current is obtained when back-EMF and voltage V_1 are in balance. Recognizing that electrical speed $\omega = \frac{d\theta}{dt}$, the electrical frequency can be written as

$$f = \frac{\omega}{2\pi} \quad (17)$$

The slope that defines the relation between the voltage magnitude and the voltage frequency is deduced from the condition that limits the rate of rise of current. Therefore, the condition to be satisfied is given by

$$V_1 = E = I_{ref} \omega L_s \quad (18)$$

Substituting (17) in condition (18), the slope V/f , is derived as

$$\frac{V_1}{f} = 2\pi I_{ref} L_s \quad (19)$$

However, when the running speed and hence also the voltage are very low, the voltage drop across the stator resistance cannot be neglected and must be compensated. The simplest stator resistance compensation method consists of boosting the stator voltage V_1 by the magnitude of the current-resistance ($I_{ref} * R$) drop (Muoz-Garcia and Novotny 1998). The compensation influence is proved as shown by Figure 6.

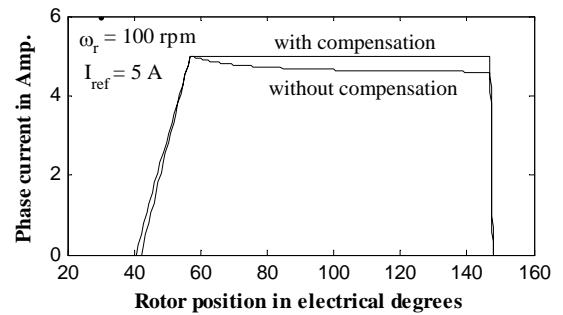


Figure 6: Current waveforms for 100 rpm without and with compensation

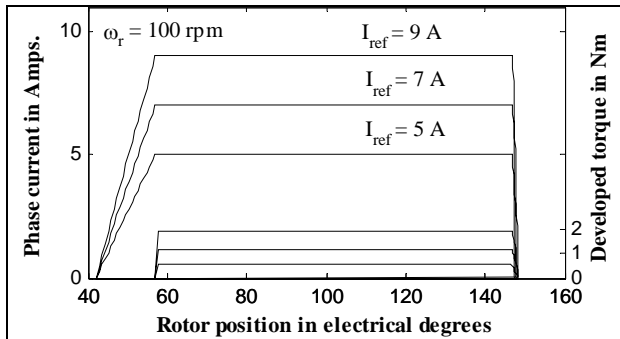
4. SIMULATION RESULTS

Simulation tests allowed initial testing of the new control concept. In addition, the objective of the simulation is to predict results that would match the experimental results such that lengthy experimental procedures can be eliminated during development stage. Simulation results are given based on comparison between V/f strategy and conventional PWM control. The motor used for simulation is a 4 kW, 8/6, four-phase SRM. The motor parameters are given in Table I.

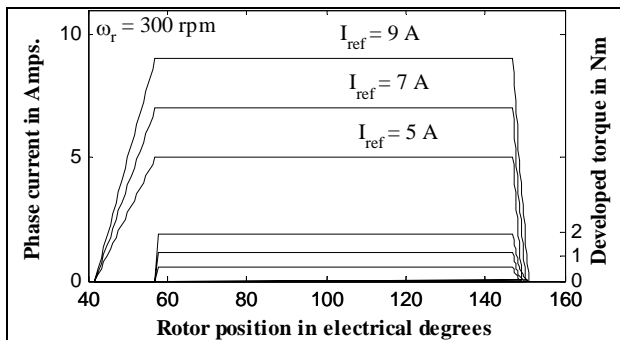
V/f and PWM control results of the SRM drive are illustrated in Figures. 7 and 8, respectively. Specifically, the phase current profile and the developed torque for various speeds and limitation levels of desired current of Figures 7 (a), 7 (b), and 7 (c) are compared to Figures 8 (a), 8 (b), and 8 (c) respectively. It is concluded that the V/f control strategy enhances significantly the phase current and the generated torque shapes.

Table 1: Four Phase, 4 kW Oulton SRM Parameters

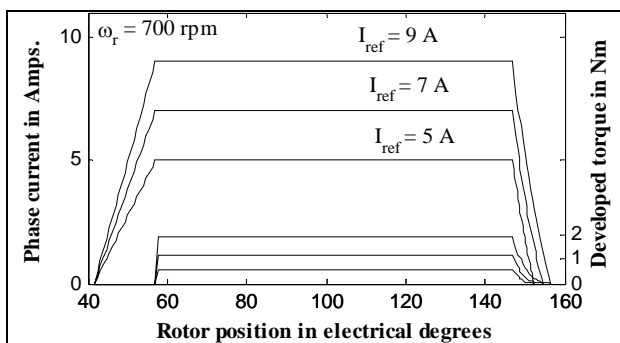
$N_s/N_r = 8/6$	Phase resistance = 0.3 Ω
$L_a = 117.8$ mH	Inertia = 0.008 Kgm^2
$L_u = 12.8$ mH	Base speed = 1500 rpm
$\beta_s = 20^\circ$	Rated voltage = 300 V
$\beta_r = 21^\circ$	RMS current = 9 A



(a)

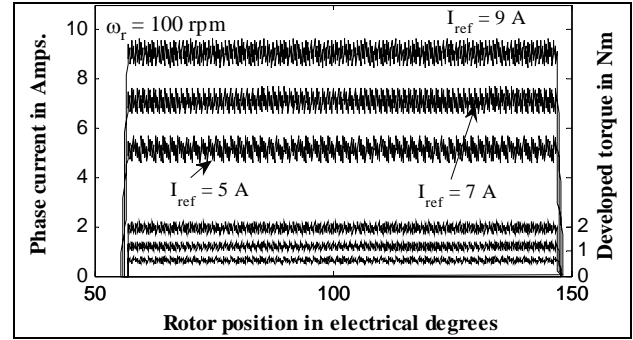


(b)

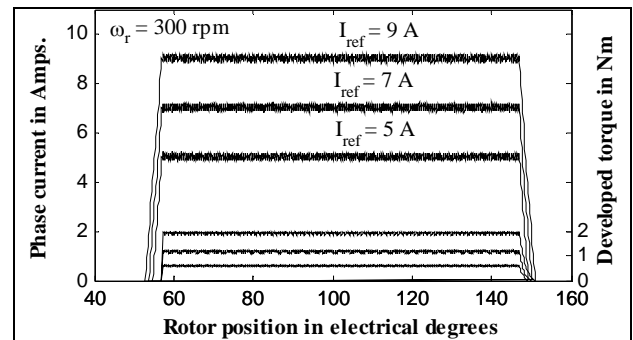


(c)

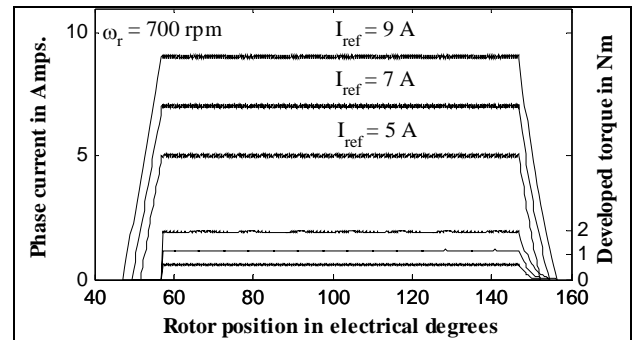
Fig. 7. The waveforms of current and torque for various current limitation values: (a) $\omega_r = 100$ rpm, (b) $\omega_r = 300$ rpm, and (c) $\omega_r = 700$ rpm with V/f control



(a)



(b)



(c)

Figure 8: The waveforms of current and torque for various current limitation values: (a) $\omega_r = 100$ rpm, (b) $\omega_r = 300$ rpm, and (c) $\omega_r = 700$ rpm with PWM control

Simulation results for phase torque and total motor torque waveforms are presented in Figure 9 for a conventional PWM mode controller, while same results for a V/f mode are shown in Figure 10. It can also be seen that the total motor torque has a low torque ripple. The impulses associated with total torque are resulting from the simple model adopted in this paper, and may be eliminated by fine tuning of the commutation angles.

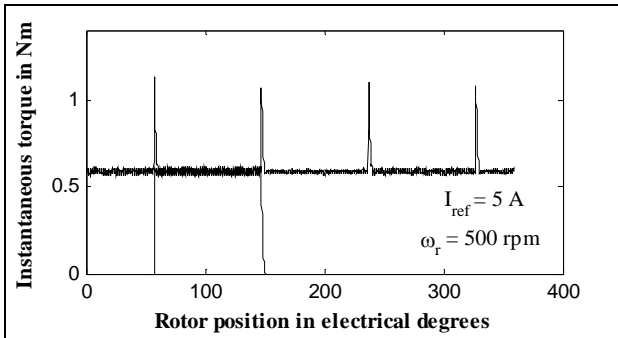


Figure 9. Phase torque and total motor torque waveforms for a PWM control

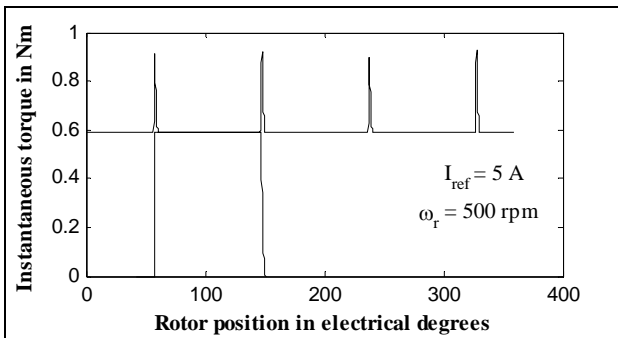


Figure 10: Phase torque and total motor torque waveforms for a V/f control

The torque-speed and the torque ripple-speed capabilities of the PWM control are illustrated by Figure 11. In order to examine the performance of the SRM with the proposed control strategy, Figure 12 displays the informative results for comparison purpose. However, the V/f produces less torque ripple in SRM developed characteristics.

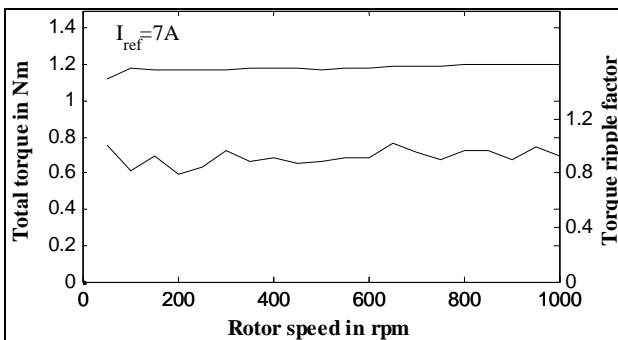


Figure 11: Variation of torque and torque ripple factor versus rotor speed for a PWM control

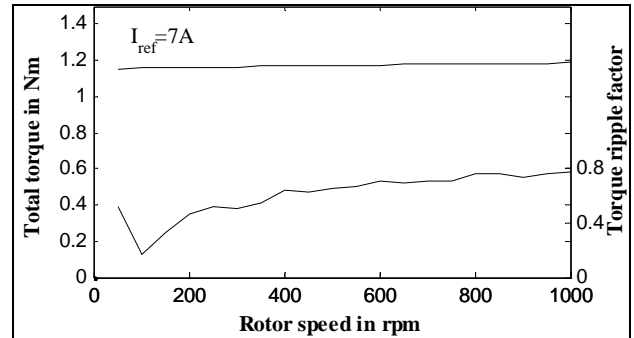


Figure 12: Variation of torque and torque ripple factor versus rotor speed for a V/f control

5. CONCLUSIONS

This paper has described V/f method capabilities for achieving a simplest and optimum control strategy for an SRM drives. Firstly, analytical solutions for winding phase current changes were determined. Then, control parameters of V/f law were selected. Simulation results are presented for SRM drive model generated with complete M-file scripts. Some important finding characteristics and current waveforms were obtained in this study, which provides theoretical basis for further development and experimental set-up. We are currently working on verifying the simulation results with the real hardware system.

REFERENCES

Cheok, A.D., and Y. Fukuda, Y., 2002, A New torque and Flux control method for Switched reluctance motor drives, *IEEE Trans. On Power Electronics*, Vol. 17, no. 4, pp. 543-556.

Christos, M., Iordanis, K., 2003, Performance optimization in switched reluctance motor drives with online commutation angle control, *IEEE Trans. On Energy Conversion*, Vol.18, no. 3, pp. 448-457.

Ertl, H., Wiesinger, T., Kolar, J.W., 2008, Active voltage balancing of DC-link electrolytic capacitors, *IET Power Electronics*, Vol. 4, pp. 488-496.

Henriques, L.O.P., et al., 2002, Review of the ripple reduction strategies in SRM, *XIV-congresso brasileiro de automatica*, pp. 1164-1169.

Kioskeridis, I., Mademlis, C., 2006, Optimal Efficiency Control of Switched Reluctance Generators, *IEEE Trans. on Power Electronics*, Vol. 4, pp. 1062-1072.

Krishnan, R., 2001, Switched Reluctance Motor Drives, *CRC Press, pp. 1-62, Cambridge, UK*.

Lee, T., et al., 2006, Control of c-dump converters fed switched reluctance motor on an automotive application, *Electric Power Systems Research 77*, pp. 804-812.

Mademlis C., Kioskeridis, I., 2007, Smooth Transition between Optimal Control Modes in Switched Reluctance Motoring and Generating Operation, *International Conference on Power Systems Transients*, pp. 1-7.

- Muño-García, A., Lipo, T.A., Novotny, D.W., 1998, A new induction motor V/f Control method capable of high-performance regulation at low speeds, *IEEE Trans. On Industry App.*, Vol. 34, no. 4, pp. 813-821.
- Pillay, P., Liu, Y., Cai, W., Sebastian, T., 1997, Multiphase operation of switched reluctance motor drives, *IEEE Industry Applications Conference* (New Orleans, USA), Vol. 1, no. 1, pp. 310-317.
- Russa, K., Husain, I., Elbuluk, M., 1997, Torque ripple minimization in switched reluctance machines over a wide speed range, *IEEE -IAS Annual Meeting*, pp. 668-675.
- Venkatesha, L., Ramanarayanan, V., 1998, Torque ripple minimization in switched reluctance motor with optimal control of phase currents, *International Conference on Power Electronic Drives and Energy Systems for Industrial Growth*, Vol. 2, pp. 529-534.
- Zai-ping, P., Ying, J., Hui, Z., 2004, Study on switched reluctance generator, *Journal of Zhejiang University Science*, Vol. 5, pp. 594-602.
- Zhang, H., Zhang, J., Gao, R., 2009, A novel method of phase current compensation for switched reluctance motor system based on finite element, *Journal of Computers*, Vol. 4, no. 10, pp. 1064-1071.

